ELSEVIER

Photochemistry and photoinduced chemical crosslinking activity of several type II commercial photoinitiators in acrylated prepolymers

Juan Segurola, Norman Allen[*], Michelle Edge, Aitor Parrondo, Ian Roberts

The Manchester Metropolitan University, Department of Chemistry and Materials, John Dalton Building, Chester Street, Manchester M1 5GD, UK

Abstract

Some of the most important commercial benzophenone and thioxanthone photoinitiators have been analysed by various spectroscopic techniques to evaluate the relationship between their photophysical properties and photoinitiation activity for photocrosslinking of commercial acrylated monomers and prepolymers. The type of electronic transitions occurring upon absorption of light are established via UV spectroscopy. Phosphorescence spectroscopy has been used to study their triplet energies and lifetimes and phosphorescence quantum yields. Microsecond flash photolysis has also been undertaken to determine the nature of the free radical semiquinone (ketyl) intermediates. The free radical intermediate decay kinetics of the different photoinitiators have also been determined, as well as the first and second order rate constants, the transient radical absorptions and radical lifetimes. Photocrosslinking studies have been undertaken by Real Time Infrared Spectroscopy (RTIR) at different photoinitiator concentrations in the presence and absence of oxygen using a low viscosity reactive diluent and a commercial resin of higher viscosity. Pendulum hardness measurements were also carried out to correlate the film hardness properties with the kinetic results obtained with RTIR. Analysis of the data shows that whilst type II initiator photoactivity is predominantly dependent upon the absorption maxima of the chromophore, structural influences play a major role in controlling the nature of the lowest excited triplet state and the formation of radical intermediates. © 1999 Elsevier Science S.A. All rights reserved.

1. Introduction

The photochemical crosslinking of coatings and inks by ultraviolet or visible light has become established technology for many industrial applications [1–5], including offset lithographic inks, flexographic inks, screen printing, metal decoration, basecoats for beverages cans [6], wood coatings [7], pigmented coatings for textile applications [8], coatings exhibiting a stereoscopic pattern [9], pigmented primary [10] and secondary optical fibre coatings [11].

Over the years, several types of photoinitiators have been developed to induce the photopolymerization or photocrosslinking of acrylated systems. Free radical photoinitiators induce a free radical chain process in which low molecular weight monomers and prepolymers are converted by the absorption of UV/Visible light into highly crosslinked films. Measurements of the rates of curing or crosslinking vary from the simplistic, such as the thumb screw test, pencil and pendulum hardness methods to the more scientific meth-

odologies involving RTIR spectroscopy [12]. The basic mechanism for any photocurable free radical system involves the formation of free radical species through the absorption of light by the photoinitiator. The active initiating radical will then add to the monomer, inducing a chain growth polymerisation and eventually termination.

Type II photoinitiators undergo a primary bimolecular process of hydrogen atom abstraction from the environment, which may be the resin itself or a solvent. However, usually amine cosynergists are used for enhanced efficiency. In this case, reaction usually occurs from the lowest excited state of the ketone and depends on the intersystem crossing (ISC) rate, the configuration of the triplet state (n,π^* or π,π^*) and its corresponding energy. Here, the excited triplet state of the ketone forms an intermediate excited electron transfer complex (exciplex) with the tertiary amine. Electron transfer occurs with the subsequent formation of radicals, the amino radical is then believed to be the main initiating radical (Fig. 1). Tertiary amines are mostly used as cosynergists, since they enhance the reactivity of type II photoinitiators. Amines can also react as oxygen scavengers and thereby help to overcome oxygen inhibition.

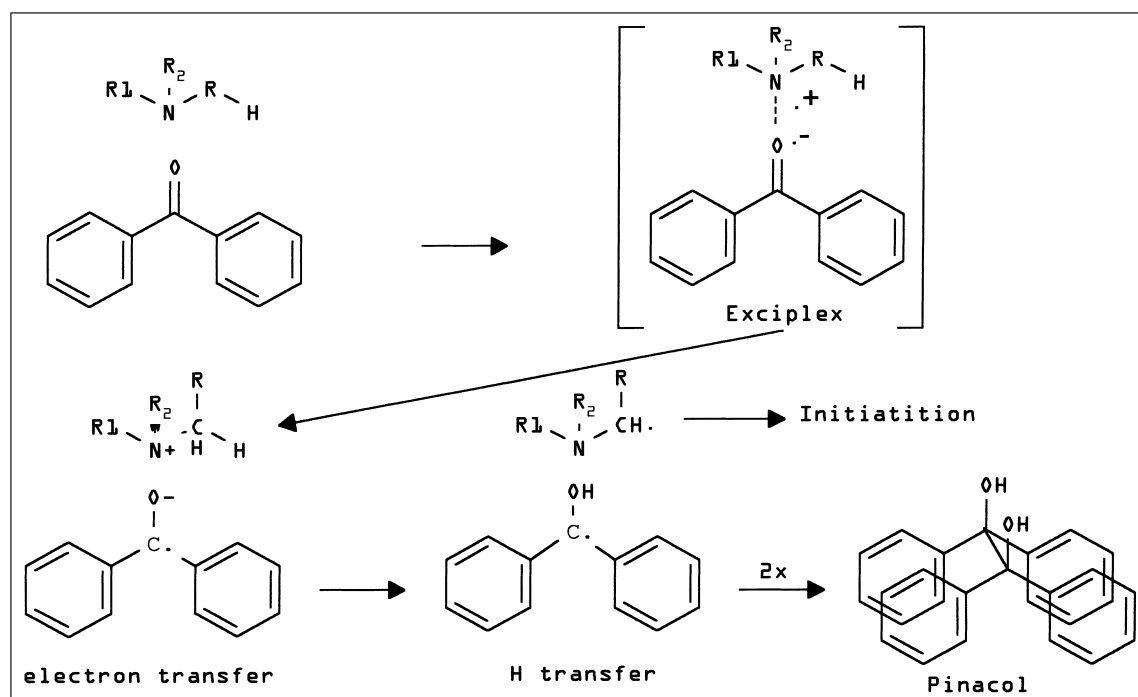*Corresponding author. Tel.: +44-161-247-1432; fax: +44-161-247-6357.

Fig. 1. Electron and hydrogen atom abstraction processes between benzophenone and an amine.

The photochemical and photophysical properties of a wide range of benzophenone [13–16] and thioxanthone [17] photoinitiators (Type II photoinitiators) have been extensively studied and reviewed [18] in the literature. Benzophenone represents the most important bimolecular photoinitiator since the use of benzophenone combined with amines makes possible the formulation of cost effective UV inks and coatings. Benzophenone is frequently used in combination with unimolecular photoinitiators (Type I) as well as with tertiary amines for enhanced reactivity. Thioxanthones are used in printing inks due to the longer wavelength absorption characteristics in the near UV range of the spectrum. They react similarly to benzophenone, but here tertiary amines must also be used. The thioxanthones are also often used in conjunction with type I photoinitiators to design cost effective synergistic photoinitiator blends.

Modification of the structure of conventional photoinitiator chromophores for improved property requirements is a subject of much interest and activity [13–17]. In this context, structures based on the thioxanthone and benzophenone chromophore have attracted intensive academic and industrial interest. As a consequence of this, several benzophenone and thioxanthone derivatives are currently used in the UV curing industry in several applications. In this study, the photocuring kinetic characteristics of the most important benzophenone and thioxanthone derivatives on the market have been compared and related to their photophysical and photochemical characteristics. This was undertaken firstly, to compare the photoactivities of the latest range of initiators and to ascertain the most important photophysical requirements in relation to their chemical structure. Whilst such

studies have been undertaken on ranges of novel esoteric non-commercial initiators no such comparative study has been undertaken on the latest commercial systems.

2. Experimental

2.1. Materials

The chemical structures of the photoinitiators, their chemical names and suppliers are shown in Table 1 and in Fig. 2. The solvents methylcyclohexane, acetonitrile and isopropanol used in this work to obtain the UV spectra were of HPLC grade quality. The reactive diluent Actilane 440 PPTTA (alkoxylated tetrafunctional acrylate monomer) was supplied by Akcros, Manchester and the resin Crodamer U2/ 297 (acrylated urethane alkyd resin in 20% GPTA or Glyceryl propoxylated triacrylate) was supplied by Croda Chemicals, Liverpool.

2.2. UV spectroscopy

Absorption spectra were obtained using a Perkin-Elmer Lambda 7 absorption spectrometer on solutions of photoinitiators in three solvents of different polarity in order to study the effect of solvent polarity on the absorption properties of photoinitiators such as hyperchromic and hypochromic effects and hypsochomic and bathochromic shifts. Methylcyclohexane, acetonitrile and isopropanol were the chosen solvents. The solutions were analysed by UV spectroscopy at different concentrations in order to obtain the

Table 1
List of photoinitiators

| Commercial name	Chemical name	Supplier
Speedcure BP	Benzophenone	Lambson
Speedcure BEM	BP/methyl–BP mixture	Lambson
Speedcure MBB	Methyl *o*-benzoylbenzoate	Lambson
Quantacure BMS	(4-(4-methylphenylthio) phenyl) phenylmethanone/4-benzoyl-4′-methyldiphenyl sulphide	G. Lakes
Esacure TZT	Eutectic mixture of 2,4,6-trimethylbenzophenone and 4-methylbenzophenone	Lamberti
Triganol 12	*p*-Phenyl benzophenone	AKZO
Quantacure ITX	Isopropylthioxanthone (mixture of 2-and 4-isomers)	G. Lakes
Quantacure CPTX	1-Chloro-4-propoxythioxanthone	G. Lakes
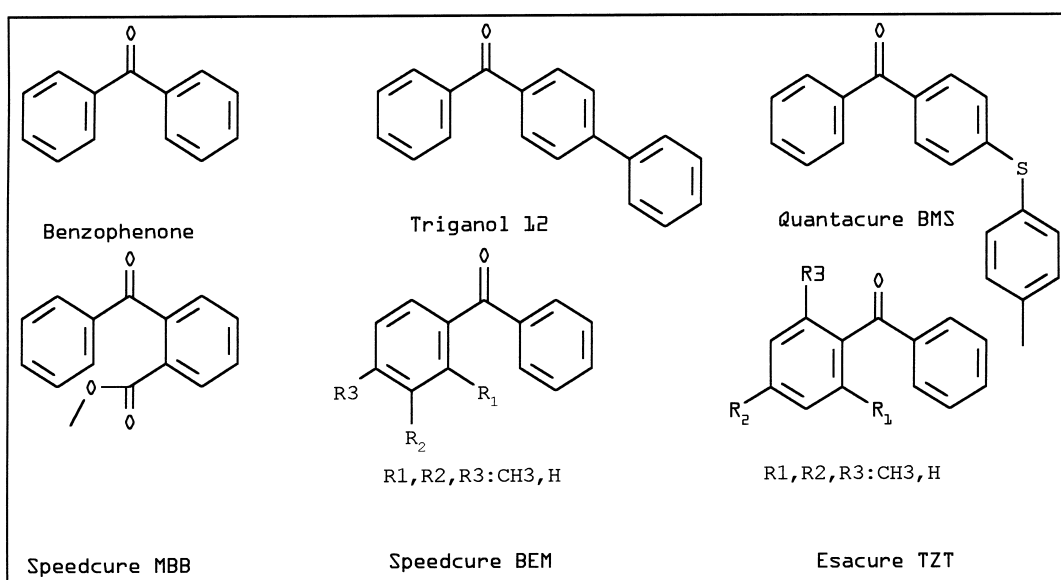
Fig. 2. Benzophenone derivatives photoinitiators (Type II).

best correlation by regression analysis. From the slope of the linear regression lines the extinction coefficients of the photoinitiators were calculated in the previously mentioned solvents.

UV spectroscopic studies were conducted using quartz cells with a path length of 1 cm. The sample in the cell was subjected to ultraviolet light between 200 and 500 nm and the approximate extinction coefficients were calculated using the Beer–Lambert's Law.

2.3. Phosphorescence measurements

Luminescence measurements are widely used by photochemists to study the photochemical processes occurring by a molecule upon the absorption of light. Phosphorescence measurements provide information related to the lowest lying excited triplet states of a molecule such as its energy, lifetime and phosphorescence quantum yield. Phosphorescence quantum yield measurements provide an idea of the relative number of molecules that emit phosphorescence radiation following the absorption of light. Since the majority of the photochemical reactions are produced from the lowest excited triplet states of a molecule, quantum yields calculations have been extensively used to investigate the photophysical and photochemical characteristics of an extensive variety of chemical systems, such as photoinitiator systems.

The determination of phosphorescence quantum yields using optically dilute solutions is the most common method currently employed [19]. Phosphorescence quantum yields ($\phi_{\text{phosphoresence X}}$) can be calculated by the relative method with the following expression [20,21].

$$\phi_{\text{phosphoresence X}} = \phi_{\text{phosphoresence R}}(A_R/A_X)$$
$$\times (\eta_X^2/\eta_R^2)(\text{Area}_X/\text{Area}_R)$$

where $\phi_{\text{phosphoresence R}}$ is the known quantum yield of the reference, A_R and A_X are the absorbance at the excitation wavelength of the reference and sample solution respectively, I_R and I_X are the intensities of the light at the excitation wavelength λ for reference and sample respectively, η_X and η_R are the refractive indices of the solvents used in the reference and sample respectively, Area_R and Area_X are the integrated areas under the corrected emission spectra.

For sample and reference it is assumed that the integrated luminescence intensity (Area$_R$ and Area$_X$) measured at 77 K is proportional to the fraction of light absorbed (A_R and A_X) measured at room temperature, all geometrical factors are identical (cells of constant path length L, reproducible positioning of cell in the instrument…), the excitation beams are monochromatic, reflection losses are the same (same cell thickness), internal reflection effects are equal – more feasible in highly diluted solutions (reabsorption and re-emission are negligible) and isotropic light is emitted.

Linear proportionality between the phosphorescence emission intensities (area measurements) and the absorbance at the excitation wavelength $\lambda = 290$ nm has been examined over a range of optical densities. Similar low absorbance values around 0.05 at the excitation wavelength $\lambda = 290$ nm in methyl cyclohexane have been used in both reference and sample in order to avoid the need for any correction factor due to the systematic error created by the power series approximation (5% systematic error for AL = 0.043) [22].

Absorbance values were obtained from more concentrated solutions of known absorbance (absorbance around 1) by diluting the sample by a certain factor. This method presented a higher accuracy than the direct spectroscopic measurement due to the error obtained when measuring low absorbance values (10% relative error is obtained when measuring the absorbance of a solution around 0.05 considering a detector sensitivity around ±0.005) [23].

The solvent selection is an important aspect, which should be considered when measuring phosphorescence quantum yields at 77 K since solvents of high purity are required for the formation of a transparent glass [24]. Traces of water should be avoided since they form non-transparent/cracked glasses. Absolute ethanol and methylcyclohexane form transparent glasses and provide reproducible results [25].

Triplet lifetimes can be calculated from the following first order rate equation:

$$\mathrm{d}I_t/\mathrm{d}t = kI_t \int \mathrm{d}I/I = \int k\mathrm{d}t \Rightarrow \ln I_t = \ln I_0 + kt$$

where I_t is the phosphorescence intensity at time t, I_0 is the phosphorescence intensity at time zero and k is kinetic constant. The triplet lifetime τ can be defined as the time required to the intensity to decrease to a value $I_\tau = 1/eI_0$. Substitution of $I_\tau = 1/eI_0$ in the equation shows that the triplet lifetime is obtained from the inverse of the kinetic constant k.

$$\ln I_t = \ln I_0 + kt \Rightarrow I_t = I_0 e^{-kt} \text{ and at } t = \tau,$$

$$I_\tau = 1/eI_0 = I_0 e^{-k\tau} \Rightarrow \tau = k^{-1}$$

Benzophenone has been used as the reference assuming a phosphorescence quantum yield of 0.74 in absolute ethanol at 77 K [19]. Phosphorescence quantum yields and triplet lifetimes were measured in methyl cyclohexane with a Perkin-Elmer LS-5 luminescence spectrometer. All the

spectra were corrected using a Perkin-Elmer IBM-compatible GEM package with an appropriate file for this purpose.

2.4. Flash photolysis measurements

The use of a flash of light to induce photochemical reaction forms the basis of flash photolysis. The concentration of transients produced in a photochemical reaction (triplets, singlets or radicals) is normally too low to be detected by their absorption spectra. The use of a high intensity flash source can populate sufficiently the excited states to produce a high enough transient concentration to be measured by absorption spectroscopy. The changes with respect to time of the intermediate concentration can be monitored from absorption measurements by flash photolysis techniques. The monitoring source is switched on and a wavelength is selected at which the species of interest absorbs radiation. The photolysis lamp is then fired and the absorbance at this wavelength is observed on an oscilloscope. The wavelength can be changed as required to measure the absorbance of the intermediates at different wavelengths of interest.

The absorption spectra of new species of the transients formed during flash photolysis are calculated from oscilloscope deflection values χ. It is assumed that the photomultiplier response is linear with respect to the light intensity. Oscilloscope deflection χ is then proportional to the light intensity I

$$I_0 = k\chi_0 \text{ and } I = k\chi$$

where k is a constant which depends on the sensitivity of the detector. It is necessary to assume the validity of the Beer–Lambert's law over the concentration region studied to calculate kinetic constants. Beer–Lambert's law can also be expressed as

$$A_\lambda = -\log T = \log(I_0/I) = \log(\chi_0/\chi) = \varepsilon_\lambda c L$$

where $T = I/I_0$ where A_λ is the absorbance of the solution at wavelength λ, ε is the molar extinction coefficient at wavelength λ and L is the optical pathlength.

This equation provides the possibility of measuring the transient absorption spectra, the transient lifetimes and the kinetic constants. Transient (triplets or radicals) decay can follow unimolecular or bimolecular processes depending on the type of initiating system. The order rate constants can be calculated by considering a first or a second order reaction mechanism:

A first order rate constant assumes that the rate of disappearance of a chemical species is proportional to its concentration (unimolecular process). Since the absorbance is proportional to the concentration of the species a first order reaction equation can be expressed by

$$\mathrm{d}A_t/\mathrm{d}t = kA_t \text{ and } \int \mathrm{d}A_t/A_t = \int k\mathrm{d}t \Rightarrow \ln A_t = \ln A_0 + kt$$

where A_t is the absorbance at time t and A_0 is the absorbance

before the flash. Plots of $\ln A_t$ versus time can be analysed and the first order rate constant can be calculated from the slope.

A second order rate constant assumes that the rate of disappearance of a chemical species (intermediate) is proportional to its concentration squared (bimolecular process). A second order reaction can be expressed by

$$dA_t/dt = kA_t^2 \text{ and } \int dA_t/A_t^2 = \int k\,dt \Rightarrow 1/A_t = 1/A_0 - kt$$

Plots of $1/A_t$ versus t can be analysed and the second order rate constant can be calculated from the slope.

The model, which provides the best correlation when measuring the regression line is considered to be the predominant decay mechanism. For first and second order models the same time range (around 0.1 ms) was measured after the flash to calculate the rate constants by regression analysis.

The lifetimes of the transient radicals can be measured for both models from their decays by measuring the time required for the transient concentration to fall to 1/e of its initial concentration. End of pulse transient absorption spectra of different photoinitiators in isopropanol ($C = 1 \times 10^{-5}$ M) on the microsecond time scale were obtained using a kinetic flash photolysis apparatus utilising two 16 k xenon filled flash lamps with 300 J energy output (operated at 10 kV) and a 150 W tungsten/halogen monitoring source. Transient decay profiles were stored using a Gould model 1425 storage oscilloscope and solutions were degassed using white spot nitrogen gas (<5 ppm O_2).

2.5. Real time infrared spectroscopy and Pendulum hardness

Different techniques have been used for measuring the reactivity and curing of UV systems. Both direct and indirect methods of analysis have been used in order to evaluate and compare the reactivity of photoinitiators. RTIR [11,12,26] is based on the decrease in the vinyl absorbance at 812 cm^{-1} during the polymerisation reaction. The sample is polymerised with UV radiation whilst the infrared beam measures the decrease of absorbance. Pendulum hardness measures the number of oscillations to decrease from 6° to 3° from the vertical, the harder the film the higher number of oscillations.

2.6. RTIR

The irradiation source used was a Xenon lamp ILC 302UV (Laser Lines) connected to a dispersive infrared spectrophotometer. A sample of a solution of a photoinitiator at 2% (w/w) in a tetrafunctional reactive diluent PPTTA was positioned between two sodium chloride salt plates covered with two pieces of low density polyethylene film using a Teflon separator to give a film thickness of 50 μ. Two polyethylene films were placed in the reference beam in order to subtract the polyethylene absorption from the sample. The effect of oxygen inhibition on the curing efficiency of a range of photoinitiators has also been evaluated. The liquid samples were applied with calibrated wire bars [27] (No 0) on sodium chloride plates to give a film thickness of 4 μ and it was positioned uncovered in the sample holder. The reactivity of several Type II photoinitiators at 8% weight at 4 μ has been performed using an acrylated polyurethane alkyd at 20% GPTA commercialised with the name Crodamer U2/297 in the presence of air.

Plots of conversion percentage and polymerisation rate versus irradiation time were obtained. The polymerisation rates were calculated from the slope of % conversion versus time plots at short irradiation times. For each sample replication has been done in order to have an estimation of the pure errors and to prevent gross errors. The results were expressed as the mean values and the standard deviations gave an indication of the spread of the results. The reactivity plots shown in the figures were averaged.

2.7. Pendulum hardness measurements

A comparative study of photoinitiator reactivity at 2% weight has also been performed on a broad range of commercial photoinitiators using PPTTA as the reactive diluent. The measurements were obtained with films of 75 μ thickness on glass. A K wired bar (No 7) was used to apply the wet films. The films were cured with a medium pressure mercury lamp of around 80 W/cm (Primarc) at 50 ft/min [28–30] (1 pass) using a tunnel conveyor. The spectral output was measured with a Solascope radiometer (Solatell) connected to a Sola-Probe. The hardness measurements were obtained after 24 h. The average number of oscillations was obtained from at least five replicate measurements and has been described elsewhere [3,4]. Measurements were obtained using a Sheenan hardness instrument (Sheenan Instruments, London).

3. Results and discussion

3.1. UV spectroscopic results

The study of the spectral absorption shifts of photoinitiators with solvents of varying polarities can help to identify the nature of the different absorption transitions occurring upon the absorption of light. The solvent polarity effect on the absorption characteristics can be explained by the different relative polarity of the ground and the excited states. The high stabilisation (reduction in energy) of non-bonding n orbitals observed with polar solvents is due to its polar nature, similarly π^* orbitals are more stabilised than are π orbitals since π^* orbitals are more polar. Such solvents shifts are due to differences in the relative capabilities of solvents to solvate the ground state of a molecule as compared with their ability to solvate the excited states.
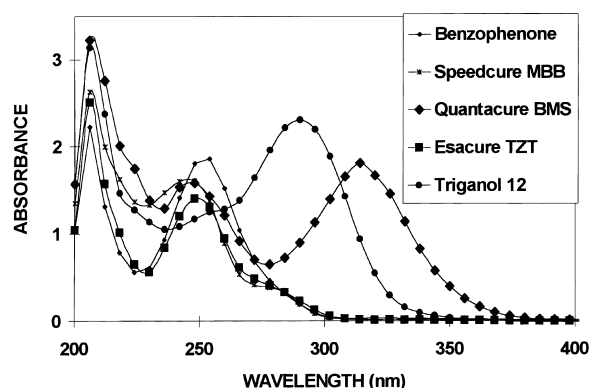
UV SPECTRA OF TYPE II PHOTOINITIATORS

Fig. 3. UV absorption spectra of photoinitiators in isopropanol ($C = 1.0 \times 10^{-4}$ M).

UV SPECTRA OF NEAR UV TYPE II PHOTOINITIATORS

Fig. 4. UV absorption spectra of photoinitiators in isopropanol ($C = 1.0 \times 10^{-4}$ M).

The most important UV transitions of the photoinitiators studied in isopropanol, acetonitrile and methylcyclohexane are shown in Figs. 3 and 4 and in Tables 2 and 3. Benzophenone derivatives exhibit a main $\pi \rightarrow \pi^*$ transition around 250 nm and a weak forbidden $n \rightarrow \pi^*$ transition around 340 nm.

The benzophenone derivative substituted in the para position by an methylphenylthio group, Quantacure BMS, is characterised by showing a strong red shifted absorption around 315 nm, since the thioether group introduces a charge transfer character into the lowest lying $\pi \rightarrow \pi^*$ transition. This increased absorption in the spectral window leads to higher photoactivity and permits its use in pigmented systems. Adversely, its strong absorption around 310–320 nm, which tails off up to 380 nm imparts a small degree of inherent yellowness to this compound and limits its application in clear coatings. Additionally, Quantacure BMS gives rise to C–S bond cleavage reactions producing alkyl and alkylthio radicals [28]. Triganol 12 also exhibits a red shifted absorption due to extension of π conjugation, because of para substitution by a phenyl group. This bathochromic effect on its $\pi \rightarrow \pi^*$ transition is accompanied by an increase in the absorption intensity (hyperchromic

effect). The lowest lying triplet state of Triganol 12 is $\pi\pi^*$ whilst that of benzophenone is $n\pi^*$.

The thioxanthone derivatives have extended absorption up to 420 nm, depending upon the type of substitution. Solvent shift data indicate a transition with a mixed $n\pi^*/\pi\pi^*$ character with little change in extinction coefficient values. In the case of thioxanthones, there is a variable red/ blue shift in the absorption maxima with increasing solvent polarity, indicative of strongly mixed $n\pi^*/\pi\pi^*$ states. CPTX shows a more pronounced red shifted maximum than ITX which may be due to the inductive effect by the chlorine atom substituted in the 1-position and by resonance by the propoxy substituent in the 4 position.

3.2. Phosphorescence results

Phosphorescence quantum yields in methylcyclohexane of the Type II photoinitiators are compared in Table 4. All the photoinitiators give rise to a high degree of intersystem crossing ISC as reflected by their high phosphorescence quantum yields. Quantacure BMS exhibits the highest phosphorescence quantum yields among all the benzophenone derivatives studied ($\phi_{p\ BMS} = 0.75$). Quantacure BMS has a

Table 2
$\pi \rightarrow \pi^*$ transition of several photoinitiators in different solvent systems

Photoinitiator	Methylcyclohexane		Acetonitrile		Isopropanol	
	λ max	log ε	λ max	log ε	λ max	log ε
Benzophenone	248.2	4.30	250.3	4.19	251.5	4.27
Speedcure MBB	239.5	4.18	243.9	4.19	245.2	4.21
Genocure MBF	252.8	4.00	254.3	4.05	253.6	4.10
Quantacure BMS	311.9	4.30	311.8	4.25	315.6	4.26
Esacure TZT	244.3	4.16	247.6	4.15	249.6	4.15
Triganol 12	283.4	4.40	288.5	4.35	289.7	4.36
Quantacure ITX	255.4	4.58	257.3	4.56	257.0	4.55
Quantacure CPTX	255.4	4.58	257.3	4.51	256.8	4.59

Table 3
$n \rightarrow \pi^*$ transition of several photoinitiators in different solvent systems

Photoinitiator	Methylcyclohexane		Acetonitrile		Isopropanol	
	λ max	log ε	λ max	log ε	λ max	log ε
Benzophenone	345.4	2.05	341.5	2.16	331.3	2.18
Speedcure MBB	335.2	1.98	332.9	2.00	326.8	2.08
Quantacure BMS						
Esacure TZT	349.3	1.91	340.0	2.04	333.3	2.07
Triganol 12						
Quantacure ITX	380.7	3.85	381.8	3.84	382.3	3.79
Quantacure CPTX	385.0	3.81	385.0	3.75	388.0	3.78

Table 4
Phosphorescence quantum yields and lifetimes of several benzophenone derivatives in methylcyclohexane

	Phosphorescence quantum yields	Lifetime (ms)
Benzophenone	0.74	5.5 (444 nm)
Triganol 12	0.68	39.8 (472 nm)
Quantacure BMS	0.75	24.5 (481 nm)
Speedcure MBB	0.61	4.2 (445 nm)
Esacure TZT	0.12	4.6 (449 nm)
Quantacure ITX	0.76	47.2 (450 nm)
Quantacure CPTX	0.43	53.6 (484 nm)

longer triplet lifetime and lower triplet energy than benzophenone in agreement with the higher polycrosslinking rate observed in the polymerisation kinetic experiments to be discussed below. On the other hand, Esacure TZT has a low phosphorescence quantum yield ($\phi_{p\ TZT} = 0.12$) and a short triplet lifetime ($\tau = 4.6$ ms; $\lambda = 449$ nm) as well as a low photocrosslinking rate in comparison to the other photoinitiators. There is a correspondence between phosphorescence quantum yields and triplet lifetimes since type II photoinitiators follow a bimolecular reaction mechanism via hydrogen atom abstraction [1] with hydrogen atom donors such as tertiary amines. Since type II photoinitiators react from their lowest lying excited triplet states it should be expected that long-lived triplets would have a higher probability to form an exciplex with a molecule in its environment. On the other hand, photoinitiators with triplet states that are prone to quenching by oxygen molecules, can

be more easily quenched than those exhibiting shorter triplet lifetimes. This could be the case of Triganol 12, which exhibits a relatively high quantum yield of phosphorescence and a long triplet lifetime. Its long triplet lifetime is accompanied with by a low triplet energy ($\tau = 39.8$ ms; $\lambda = 472$ nm) which diminishes its hydrogen atom abstraction capability. Triplet states with lifetimes in the range 10–100 ms tend to be primarily of a mixed $n\pi^*/\pi\pi^*$ character.

CPTX displays a lower phosphorescence quantum yield and a longer lived red shifted triplet state ($\phi_p = 0.43$, $\tau = 53.6$ ms, $\lambda = 484$ nm) than ITX ($\phi_p = 0.76$, $\tau = 47.2$ ms, $\lambda = 450$ nm) in methylcyclohexane.

3.3. Flash photolysis results

End of pulse transient absorption spectra of the photoinitiators in isopropanol are compared in Table 5 and in Figs. 5 and 6 where absorption maxima and the first and second order rate constants are compared and recorded. Benzophenone exhibits a higher maximum transient absorption spectrum than its derivatives, resulting from the formation of a high concentration of transient intermediates. The spectrum of benzophenone is normally assigned to that of the ketyl radical formed by abstraction of a hydrogen atom by the excited triplet state from isopropanol. Quantacure BMS ((4-(4-methylphenylthio) phenyl)phenylmethanone) and Triganol 12 (*p*-phenyl benzophenone) exhibit red shifted absorption spectra and lower maxima absorptivity. Speedcure MBB (methyl *o*-benzoylbenzoate) also exhibits a red shifted absorption maximum with a slightly lower maximum absorptivity than benzophenone. The methylated

Table 5
First and second order kinetic results by microsecond flash photolysis in isopropanol ($C = 1 \times 10^{-5}$ M)

	Maximum absorbance by flash photolysis	K_1 (s^{-1})	τ_1 (s)	Regression	K_2 (s^{-1})	τ_2 (s)	Regression
Benzophenone	0.546 (320 nm)	18.68	0.054	0.967	110.30	0.009	0.994
Triganol 12	0.230 (340 nm)	29.37	0.034	0.966	662.68	0.001$_5$	0.985
Quantacure BMS	0.143 (360 nm)	41.03	0.024	0.988	635.99	0.001$_6$	0.977
Speedcure MBB	0.470 (340 nm)	19.18	0.052	0.986	115.25	0.009	0.985
Esacure TZT	0.265 (320 nm)	15.19	0.066	0.981	141.49	0.007	0.990
Quantacure ITX	0.019 (380 nm)	15.23	0.066	0.980	1485.80	0.0007	0.956
Quantacure CPTX	0.0136 (370 nm)	8.822	0.113	0.962	1065.9	0.0009	0.933

END OF PULSE TRANSIENT ABSORPTION SPECTRA OF
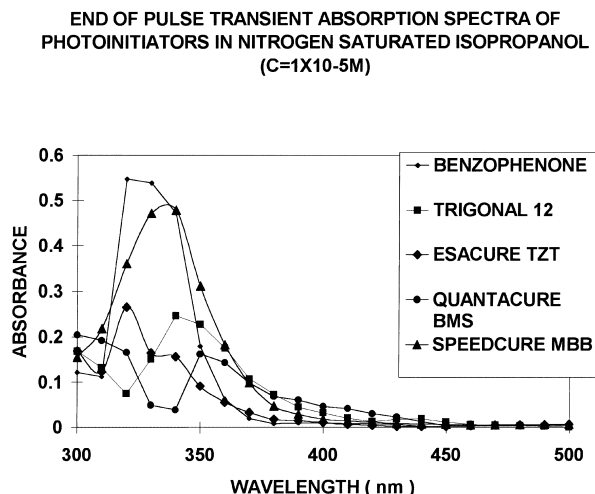PHOTOINITIATORS IN NITROGEN SATURATED ISOPROPANOL
(C=1X10-5M)

Fig. 5. End of pulse transient absorption spectra of type II photoinitiators in nitrogen saturated isopropanol ($C = 1 \times 10^{-5}$ M) produced on microsecond flash photolysis.

END OF PULSE TRANSIENT ABSORPTION SPECTRA OF
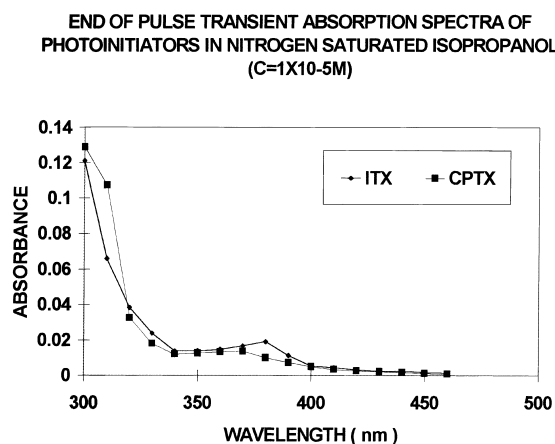PHOTOINITIATORS IN NITROGEN SATURATED ISOPROPANOL
(C=1X10-5M)

Fig. 6. End of pulse transient absorption spectra of ITX and CPTX in nitrogen saturated isopropanol ($C = 1 \times 10^{-5}$ M) produced on microsecond flash photolysis.

benzophenone, Esacure TZT, does not exhibit an absorption shift, but exhibits a two fold lower absorbance than benzophenone and hence a lower radical transient formation mainly due to intramolecular hydrogen atom abstraction from the ortho methyl substituent. This effect will also rapidly deactivate the excited triplet-state of the benzophenone chromophore and reduce the triplet quantum yield, as is the case in Table 4. The intensity of transient formation follows this sequential order:

BP > MBB > TZT > T12 > BMS > ITX > CPTX

The majority of the photoinitiators studied follow a second order kinetic decay mechanism evidenced by regression analysis. Some photoinitiators such as Quantacure BMS and Speedcure MBB also give transients that follow a first order kinetic decay since, by instance, C–S [28] and C–O [15] bond cleavage occur upon absorption of light. CPTX also follows a unimolecular deactivation mechanism

since dehalogenation (C–Cl bond cleavage) occurs as indicated by earlier solution photolysis studies [16].

Benzophenone, Triganol 12 and Esacure TZT exhibit a bimolecular deactivation mechanism for the transient radical. The second order lifetimes of the radical intermediates were calculated and followed the order:

BP > MBB > TZT > BMS $\cong$ T12 > CPTX > ITX

Consequently, benzophenone derivatives present longer radical intermediate lifetimes than the thioxanthones studied supposing a bimolecular deactivation mechanism. Additionally, benzophenone exhibits a longer-lived ketyl radical than its derivatives, presenting a certain correlation with the kinetic measurements carried out by RTIR where benzophenone gave higher photocrosslinking rates than Esacure TZT, Triganol 12 and Speedcure MBB.

On the other hand, supposing the transient decay follows a first order kinetic decay mechanism the lifetimes of the radical intermediates would have an opposite tendency than in a second order mechanism. The radical intermediate lifetimes follow this order:

CPTX > TZT $\cong$ ITX > BP $\cong$ MBB > T12 > BMS

The higher radical lifetime of CPTX in comparison to ITX can be responsible for the higher photocrosslinking rate of CPTX observed in photopolymerisation experiments [16]. The narrow absorption bands with maxima at 370 and 380 nm for CPTX and ITX respectively reflect a higher ketyl radical formation for ITX than for CPTX, formed by abstraction of a hydrogen atom from the solvent by the excited triplet state of the thioxanthone chromophore [31,32].

3.4. Photocrosslinking results

The photoreactivity of some type II photoinitiators is compared in Tables 6 and 7 and in Figs. 7 and 8. Quantacure BMS displayed the highest photoinitiation activity (photocrosslinking rate) both in the presence and in the absence of air. These kinetics results were in agreement with the pendulum hardness measurements.

Benzophenone and Speedcure BEM (eutectic mixture of benzophenone and methylated benzophenones) had similar polymerisation rates and final percentage conversion. Esa-

Table 6
Reactivity of photoinitiators at 8% (w/w) in Crodamer U2/297 by RTIR in the presence of air (uncovered method)

Photoinitiators at 8% in Crodamer U2/297	R_p maximum (mol l^{-1} s^{-1})$\pm$SD	% Conversion at 25s $\pm$ SD	No. runs
Benzophenone	0.0103 $\pm$ 0.0002	19.6 $\pm$ 0.6	3
Speedcure MBB	0.0061 $\pm$ 0.0009	11.3 $\pm$ 0.6	3
Quantacure BMS	0.0114 $\pm$ 0.0001	23.9 $\pm$ 0.8	3
Esacure TZT	0.0057 $\pm$ 0.0003	11.7 $\pm$ 2.2	4
Triganol 12	0.0050 $\pm$ 0.0001	9.1 $\pm$ 0.4	3
Speedcure BEM	0.0099 $\pm$ 0.0003	20.8 $\pm$ 1.1	3

Table 7
Reactivity of photoinitiators at 2% (w/w) in PPTTA by RTIR at 50 microns (covered method) in the absence of air and pendulum hardness measurements of coatings cured at 50 ft/min with a film thickness of 75 μ (measured after 24 h)

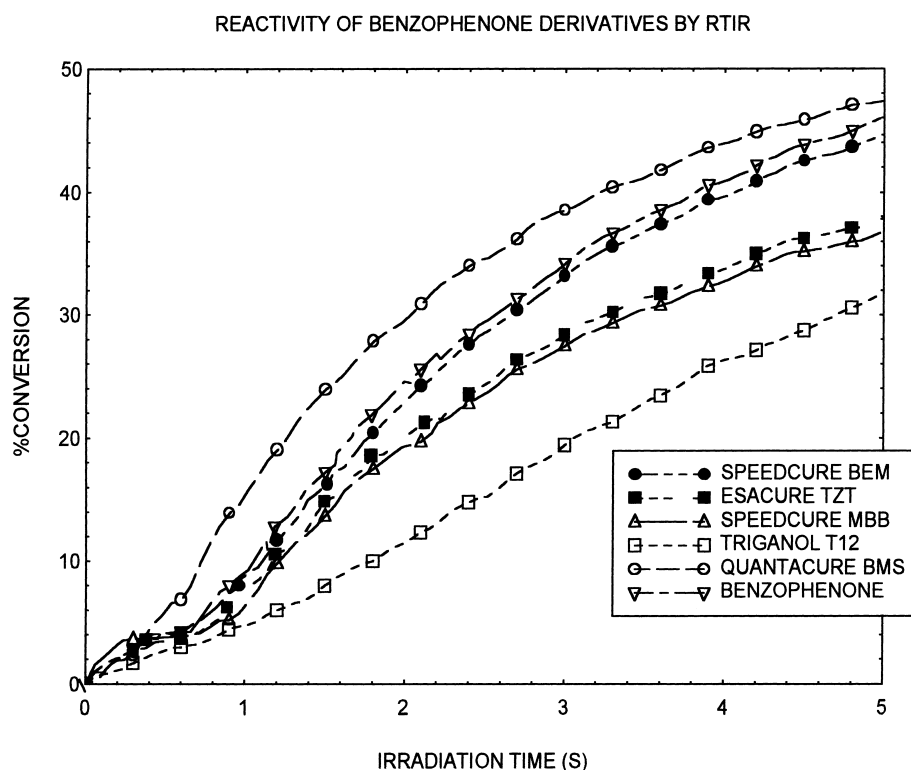| Photoinitiators at 2% in PPTTA	R_p maximum (mol l^{-1} s^{-1})$\pm$SD	% Conversion at 15 s $\pm$ SD	No of oscillations $\pm$ SD (5 runs)	No. of runs
Benzophenone	0.133 ± 0.041	62.0 ± 5.7	49 ± 14	2
Speedcure MBB	0.111 ± 0.052	56.0 ± 7.3	25 ± 7	2
Quantacure BMS	0.146 ± 0.053	64.9 ± 8.5	75 ± 5	3
Esacure TZT	0.121 ± 0.044	52.8 ± 9.4	26 ± 3	2
Triganol 12	0.053 ± 0.021	57.1 ± 5.8	No cured	2
Speedcure BEM	0.132 ± 0.042	61.8 ± 4.81	47 ± 12	2

Fig. 7. Reactivity of several benzophenone derivatives at 2% (w/w) in PPTTA at 50 μ in the absence of air.
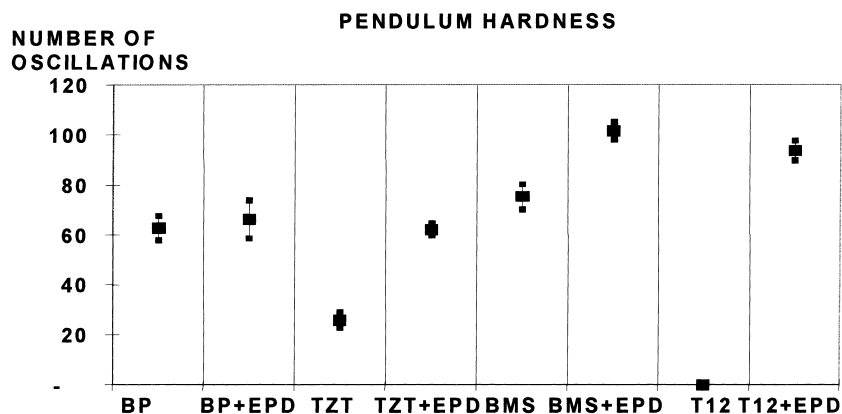

Fig. 8. Pendulum hardness of PPTTA films photopolymerised using benzophenone type derivatives (2%, w/w) alone and with the addition of the tertiary amine EPD at 2% (w/w).
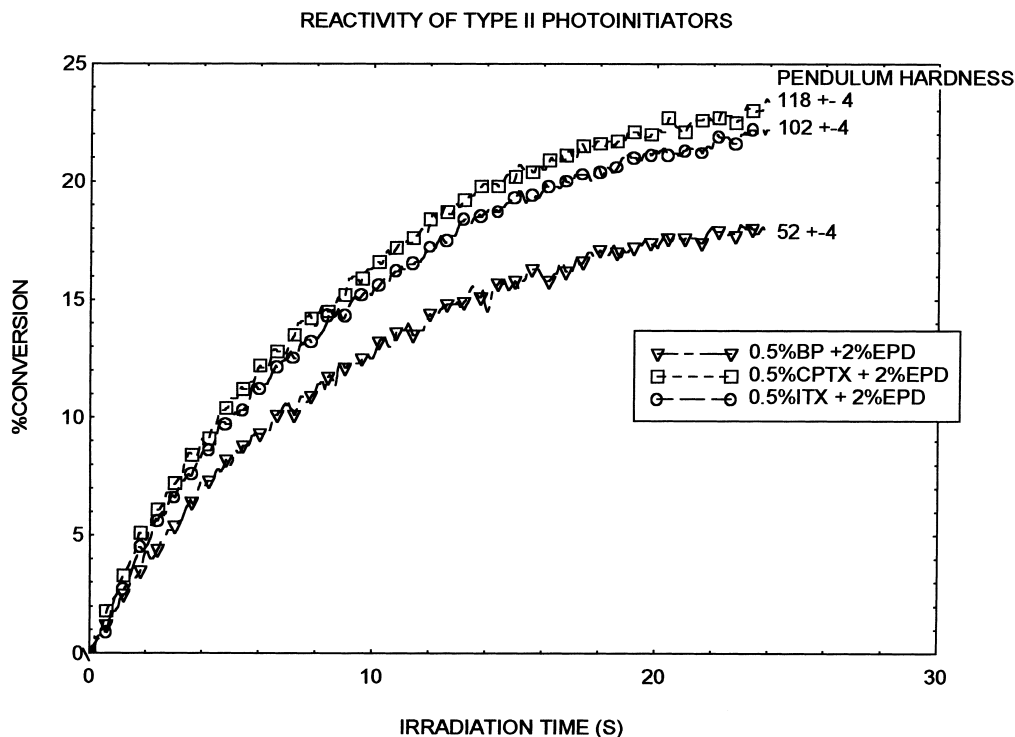
REACTIVITY OF TYPE II PHOTOINITIATORS

Fig. 9. Reactivity of benzophenone, ITX and CPTX at 2% EPD at 50 microns in PPTTA in the absence of air.

cure TZT gave lower reactivity than benzophenone and Esacure BEM in the absence of a tertiary amine despite having a similar composition. Norrish Type II intramolecular hydrogen atom abstraction may occur from the methyl group in the ortho position. On the other hand, Esacure TZT showed enhanced reactivity in the presence of a tertiary amine showing similar hardness properties to benzophenone (Fig. 8).

Genocure MBB (Methyl *o*-benzoylbenzoate) gave similar results to that of Esacure TZT. Substitution of benzophenone by an ester group in the ortho position decreased its reactivity by a factor of two, in the absence of an amine co-synergist. Triganol 12 (paraphenylbenzophenone) gave the poorest results in the absence of an amine exhibiting very low polymerisation rates and poorly cured films. Its low reactivity results from a lower hydrogen atom abstraction ability resulting from the lower energy of its triplet state due to a charge transfer by the phenyl group in the para position. Its photoreactivity is increased dramatically in the presence of an efficient electron proton donor such as a tertiary amine giving harder films than films cured with benzophenone (Fig. 8).

CPTX exhibited a higher reactivity and hardness than ITX in the presence of an amine. CPTX and ITX exhibited a higher kinetic reactivity and gave harder films than benzophenone (Fig. 9). On the other hand, other experiments evidenced that ITX has a higher reactivity than CPTX in the absence of an amine, due to the lowest triplet state of CPTX resulting in a lower energy n–π^* transition by charge transfer and a consequent lower hydrogen atom abstraction ability.

4. Conclusions

The photocrosslinking activities of benzophenone and thioxanthone derivatives are highly dependent upon the degree of substitution of the chromophore, which controls the degree of charge transfer content and the energy of the lowest lying triplet state. Reaction of the photoinitiators occurs by ketyl radical formation due to either electron or proton abstraction in the presence of an efficient donor such as a tertiary amine or by direct hydrogen atom abstraction from the photoexcited triplet state of the chromophore.

Quantacure BMS exhibits a higher polymerisation rate than the other benzophenone derivatives studied due to the charge transfer character of the methylphenylthio substituent and its extended absorption in the near ultraviolet range. The unsubstituted benzophenone shows higher reactivity than its methyl ester derivative Speedcure MBB and than its phenyl derivative Triganol 12 in the absence of an amine. Speedcure BEM shows a similar reactivity to that of benzophenone and a higher reactivity than its similar counterpart Esacure TZT. Since Esacure TZT is substituted in the ortho position by a methyl group it may exhibit a Norrish Type II intramolecular hydrogen atom abstraction process which will reduce the photoactivity of the lowest excited triplet state of the chromophore toward intermolecular hydrogen atom abstraction.

CPTX showed higher photoreactivity than ITX as reflected by its higher polymerisation rate and hardness. Dehalogenation on photolysis can be responsible for the observed enhanced reactivity of CPTX since the chlorine

atom can either form a chloride anion and a thioxanthonyl radical or form an intramolecular hydrogen bond and produce amine hydrochloride and a thioxanthyl radical for further reaction [16].

References

[1] S.P. Pappas (Ed.), UV Curing: Science and Technology. Technology Marketing Corporation, Stanford, CT, USA, 1978.

[2] C.G. Roffey, Photopolymerisation of Surface Coatings, Wiley, New York, USA, 1982.

[3] P.K.T. Oldring (Ed.), Chemistry and Technology of UV and EB Formulation of Coatings, Inks and Paints, SITA Technology, London, UK, 1991, pp. 1–6.

[4] R. Holman, P.K.T. Oldring (Eds.), UV and EB Curing Formulation for Printing Inks, Coatings and Paints, SITA Technology, London, UK, 1988.

[5] N.S. Allen (Ed.), Photopolymerisation and Photoimaging Science and Technology, Elsevier, London, UK, 1986.

[6] T. Limure, Proceedings Conference Radiation Curing Asia, 1988, p. 461.

[7] M. Marsman, A. Luiken, R.B.M. Holweg, Proceedings Conference Radtech Europe, 1991, p. 440.

[8] K. Yoshiyuki, M. Kayuzuki, S. Toshio, M. Mitsuhiro, M. Hiromi, U.S. Patent 5013768, 1989.

[9] P. Borzel, E. Haring, German Patent Application 3304524, 1983.

[10] K.P. Murray, T.E. Bishop, Int. Patent Application WO 90/13579, 1989.

[11] R. Phillips, J. Oil Colour Chem. Assoc. 6 (1978) 233.

[12] G.L. Collins, D.A. Young, J.R. Costanza, J. Coat. Technology, 48, 1976.

[13] N.S. Allen, E. Lam, E.M. Howells, A. Green, P.N. Green, F. Catalina, C. Peinado, J. Photochem. Photobiol. A: Chem. 54 (1990) 367–388.

[14] N.S. Allen, F. Catalina, J.L. Mateo, R. Sastre, P.N. Green, W.A. Green, J. Photochem. Photobiol. A: Chem. 44 (1988) 171.

[15] N.S. Allen, S.J. Hardy, A. Jacobine, D.M. Glaser, B. Jang, D. Wolf, F. Catalina, S. Navaratnam, B.J. Parsons, J. Appl. Polym. Sci. 42 (1991) 1169.

[16] N.S. Allen, D. Mallon, A. Timms, W.A. Green, F. Catalina, T. Corrales, S. Navaratnam, B.J. parsons, J. Chem. Soc. Faraday Trans. 90(1) (1994) 83–92.

[17] N.S. Allen, F. Catalina, W. Chen, J.L. Gardette, P.N. Green, W.A. Green, K.O. Fatinikun, Eur. Polym. J. 24(5) (1988) 435–440.

[18] J.P. Fouassier, D. Ruhlman, B. Graft, F. Morlet-Savary, W. Wieder, Prog. Organic Coatings 25 (1995) 235–271.

[19] J.N. Demas, G.A. Crosby, J. Phys. Chem. 75 (1971) 991.

[20] H.V. Drushel, A.L. Sommers, R.C. Cox, Anal. Chem. 35 (1963) 2166.

[21] C.A. Parker, W.T. Rees, Analyst (London) 85 (1960) 587.

[22] J.N. Demas, G.A. Crosby, J. Phys. Chem. 75 (1971) 991.

[23] J.N. Demas, G.A. Crosby, J. Phys. Chem. 75 (1971) 991.

[24] A.T. Rhys Williams, An Introduction to Phosphorescence Spectroscopy, Perkin-Elmer, UK, 1981.

[25] J.N. Demas, G.A. Crosby, J. Phys. Chem. 75 (1971) 991.

[26] R. Phillips, J. Oil Colour Chem. Assoc. 6 (1978) 233.

[27] T.R. Kerchiss, Poly. Paint Colour J. 182 (1992) 566.

[28] W.A. Green, RadTech Asia'95 Symposium and Workshop, Thailand, 1995, p. 272.

[29] S.P. Pappas (Ed.), UV Curing Science and Technology, 2nd ed., Technology Marketing Corp., Stanford, CT, USA, 1985, pp. 3–25.

[30] W.A. Green, RadTech Asia'95 Symposium and Workshop, Thailand, 1995, p. 272.

[31] N.S. Allen, F. Catalina, P.N. Green, W.A. Green, Eur. Polym. J. 21 (1985) 841.

[32] N.S. Allen, D. Mallon, F. Catalina, A.W. Timms, W.A. Green, Eur. Polym. J. 28 (1992) 647.